Field-Induced Magnonic Liquid in the 3D Spin-Dimerized Antiferromagnet $Sr_3Cr_2O_8$

Zhe Wang,[1] D. L. Quintero-Castro,[2] S. Zherlitsyn,[3] S. Yasin,[3] Y. Skourski,[3] A. T. M. N. Islam,[2] B. Lake,[2,4] J. Deisenhofer,[1] and A. Loidl[1]

[1]*Experimental Physics V, Center for Electronic Correlations and Magnetism, Institute of Physics, University of Augsburg, D-86135 Augsburg, Germany*

[2]*Helmholtz-Zentrum Berlin für Materialien und Energie, D-14109 Berlin, Germany*

[3]*Hochfeld-Magnetlabor Dresden (HLD-EMFL), Helmholtz-Zentrum Dresden-Rossendorf, D-01314 Dresden, Germany*

[4]*Institut für Festkörperphysik, Technische Universität Berlin, D-10623 Berlin, Germany*

(Received 13 November 2015; published 4 April 2016)

We report on ultrasound and magnetization studies in three-dimensional, spin-dimerized $Sr_3Cr_2O_8$ as a function of temperature and external magnetic field up to 61 T. It is well established [A. A. Aczel *et al.*, Phys. Rev. Lett. 103, 207203 (2009)] that this system exhibits a magnonic-superfluid phase between 30 and 60 T and below 8 K. By mapping ultrasound and magnetization anomalies as a function of magnetic field and temperature we establish that this superfluid phase is embedded in a domelike phase regime of a high-temperature magnonic liquid extending up to 18 K. Compared to thermodynamic results, our study indicates that the magnonic liquid could be characterized by an Ising-like order but has lost the coherence of the transverse components.

DOI: 10.1103/PhysRevLett.116.147201

Exotic quantum spin states can be induced by magnetic fields, such as a Tomonaga-Luttinger liquid in quantum-spin ladders [1–3], or a long-range canted-XY antiferromagnetic order in spin-dimerized quantum magnets [4–8]. In dimerized spin-1/2 quantum antiferromagnets, spin dimers formed by pairs of $S = 1/2$ magnetic ions can weakly couple along preferred directions as in $(C_5H_{12}N)_2CuBr_4$ [2,3] and $TlCuCl_3$ [6,7], in layers, e.g., in $SrCu_2(BO_3)_2$ [9,10] and $CuTe_2O_5$ [11,12], or in a three-dimensional network as in $Ba_3Cr_2O_8$ and $Sr_3Cr_2O_8$ [13–20]. The ground state of these systems is a quantum disordered paramagnet with gapped elementary magnon (singlet-triplet) excitations (spin-1 bosons).

If dimer-dimer interactions can be neglected, a quantum phase transition from the quantum disordered (QD) phase to a ferromagnetic (FM) state can be induced by an external magnetic field when the Zeeman energy compensates the intradimer interactions. This transition is reflected by a steplike increase between two magnetization plateaus with zero and fully saturated moments, respectively. The former corresponds to the quantum disordered paramagnet, the latter to the induced ferromagnetic state. This steplike increase can be smoothed by interdimer interactions and the paramagnetic and ferromagnetic states are separated by an ordered three-dimensional (3D) canted-XY antiferromagnetic (AFM) phase. In this case, the quantum phase transition occurs when the spin gap is closed via a linear Zeeman interaction [Fig. 1(c)]. At the critical field the spin Hamiltonian can be mapped onto a boson lattice model, and hence, the quantum phase transition is often discussed in the context of a magnonic Bose-Einstein condensation [4,5]: the 3D canted-XY AFM phase can be viewed as a magnonic superfluid with the number of magnons derived from the S^z component while the condensate wave function corresponds to the transverse magnetic $\langle S_i^x + iS_i^y \rangle$ order [5].

The interdimer exchange interaction plays an important role in $Sr_3Cr_2O_8$: magnon bands with a significantly large bandwidth $\sim 0.6J_0$ are observed [Fig. 1(a)] and the spin gap Δ is reduced to 2/3 of the intradimer exchange $J_0 = 5.55$ meV [21]. The magnon dispersion relation can be described by taking into account the 3D arrangement of the spin dimers [Fig. 1(b)] [18]. The dimers, each consisting of two $S = 1/2$ Cr^{5+} ions, form a triangular lattice in the crystallographic ab layers stacked along the c direction in a hexagonal structure [20,22,23]. A field-induced quantum phase transition was observed at a lower critical field $H_{c1} = 30.4$ T, corresponding to the closing of the spin gap. The phase boundary close to H_{c1} follows a critical law $T_c \sim (H - H_{c1})^{\phi}$ with an exponent $\phi = 2/3$ belonging to the universality class characteristic of the magnonic Bose-Einstein condensation [Fig. 1(c)] [17]. An upper critical field $H_{c2} = 62$ T was determined at the onset of the field-induced ferromagnet. The 3D canted-XY AFM order, which can be described by a magnonic Bose-Einstein condensation phase, exists in a domelike structure with a maximum temperature of 8 K at 44 T [17].

In a two-leg spin-ladder antiferromagnet, spin dimers forming rungs of the ladder are weakly coupled along the ladder due to interdimer interactions. An even weaker interaction between neighboring spin ladders can stabilize a 3D XY AFM order at low temperatures and high magnetic fields. Above the 3D ordered phase a 1D Tomonaga-Luttinger liquid has been identified, below a characteristic

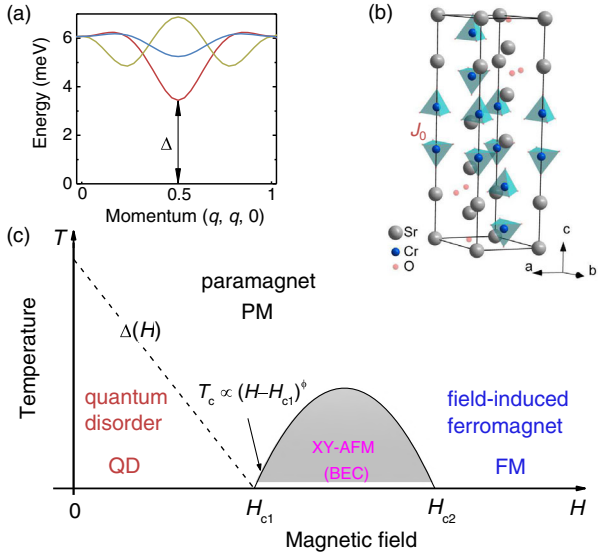

FIG. 1. (a) Dispersion relation of spin singlet-triplet excitations ($S = 1$ magnons). Δ is the spin gap at the Brillouin zone boundary (0.5,0.5,0). The dispersion relations due to three different crystallographic domains were observed by inelastic neutron scattering [18,21]. (b) The hexagonal unit cell of $Sr_3Cr_2O_8$. The spin dimer consists of two CrO_4 tetrahedra along the crystallographic c direction. J_0 is the intradimer exchange [20]. (c) (T, H) phase diagram showing paramagnetic, quantum disordered, field-induced ferromagnetic, and canted-XY antiferromagnetic phases. The phase boundary close to the quantum critical point at H_{c1} follows the power law of the universality class of the magnonic Bose-Einstein condensation with a universal exponent $\phi = 2/3$ [4,5].

temperature that is determined by the interdimer exchange along the ladder [1–3]. Above this temperature, the system enters a high-temperature paramagnetic (PM) phase [1]. Motivated by this result, we thought it worthwhile to search for a similar exotic liquid phase of magnons in the 3D system $Sr_3Cr_2O_8$.

Here, by performing ultrasound and magnetization experiments on the spin-dimerized quantum antiferromagnet $Sr_3Cr_2O_8$ in high magnetic fields up to 61 T as a function of temperature, we provide experimental evidence for the existence of a magnonic liquid phase above the 3D XY AFM dome. Softening of the acoustic modes and distinct anomalies are observed at the phase boundaries to the magnonic liquid. The phase boundaries are confirmed also by the high-field magnetization measurements.

High-quality $Sr_3Cr_2O_8$ single crystals were grown by the floating-zone method as described in Ref. [23] and were studied by neutron scattering, electron spin resonance, and infrared and Raman spectroscopy [18,19,21,24,25]. In this work the elastic properties were investigated by measurements of the velocity and attenuation of longitudinal sound waves with wave vector $\mathbf{k}$ and polarization $\mathbf{u}$ parallel to and perpendicular to the dimer orientation c, i.e., $\mathbf{k}\|\mathbf{u}\|c$ and $\mathbf{k}\|\mathbf{u}\|[1,2,0]$, which for the hexagonal structure correspond to the tensile elastic constants c_{33} and c_{11}, respectively [26]. Transverse sound waves with $\mathbf{k}\|c$ and $\mathbf{u}\|a$ corresponding to the shear elastic constant c_{44} were also utilized to study the magnetoelastic properties. The field-dependent behavior is represented by the relative sound velocity $\Delta v/v(H) \equiv [v(H) - v(0)]/v(0)$ as a function of the applied magnetic field H. A pulse-echo method with phase-sensitive detection was used [27], which allows us to detect structural and magnetic phase transitions in static as well as in pulsed fields [9,28–30]. The field-dependent measurements of the ultrasound velocity and magnetization were performed at the Dresden High Magnetic Field Laboratory in pulsed magnetic fields up to 61 T and 58 T, respectively, in the temperature range from 1.5 to 31 K. The pulsed fields for the magnetization measurements had a rise time of 7 ms and a pulse duration of 20 ms, while they were 33 and 150 ms, respectively, for the ultrasound measurements.

Figure 2(a) shows the high-field magnetization of $Sr_3Cr_2O_8$ measured at various temperatures for the magnetic field parallel to the crystallographic c axis $H\|c$. At 1.5 K, the clear onset of finite magnetization at $H_{c1} = 30.9$ T corresponds to the closing of the spin gap and the formation of a magnonic superfluid [17,18]. Above H_{c1} the magnetization increases continuously with increasing magnetic field, indicating a continuous increase of magnon density. The absence of any magnetization plateaus

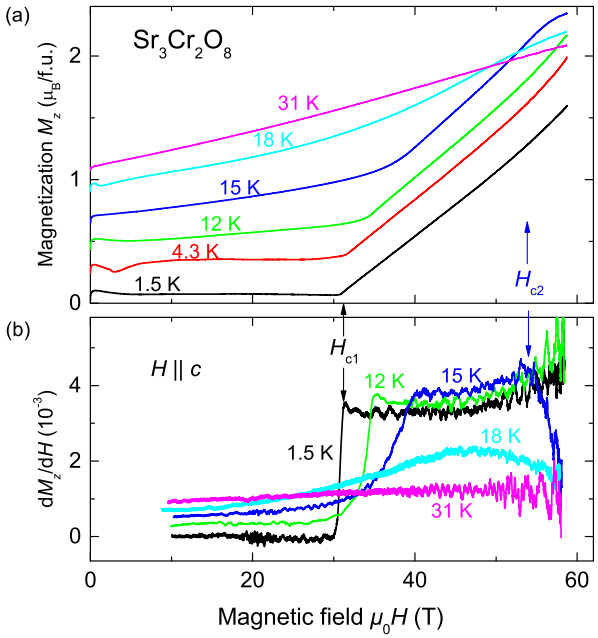

FIG. 2. (a) Magnetization M_z as a function of magnetic field along the c axis ($H\|c$) at various temperatures. The curves at higher temperatures are shifted upward by a constant of $0.22\mu_B$/f.u. for clarity. (b) Field derivative of the magnetization dM_z/dH versus magnetic field. The lower critical field H_{c1} is marked by arrows for 1.5 K. The upper critical field H_{c2} is marked for 15 K.

suggests that the kinetic energy of the magnons is dominant compared to their repulsions [5]. The saturated magnetization with an expected value of $1.98\mu_B$ per formula unit (f.u.) cannot be reached, because the upper critical field H_{c2} is out of the field range of this experiment [17,18]. The critical field H_{c1} is well defined by the field derivative of the magnetization as shown in Fig. 2(b). At 1.5 K a steplike discontinuity of the field derivative indicates H_{c1}. With increasing temperature up to 15 K, the onset of magnetization becomes less pronounced and shifts to higher values, while the upper critical field H_{c2} is expected to shift towards lower fields. And indeed, at 15 K the magnetization levels off slightly above 50 T. At 18 K the field derivative of the magnetization becomes significantly reduced with a broad maximum at 48 T [Fig. 2(b)]. At 31 K the magnetization increases linearly with magnetic field, characteristic of the paramagnetic phase.

Figure 3(a) shows the relative sound velocity $\Delta v/v$ of the elastic mode c_{11} as a function of magnetic field parallel to the c axis ($H\|c$) at various temperatures. This mode is very sensitive to the field-induced phase transitions. At 4.2 K with increasing magnetic fields, c_{11} shows a small steplike decrease at H_{c1}, softens continuously with increasing slope, and finally hardens abruptly at H_{c2} exhibiting a sharp minimum. Similar anomalies at H_{c1} and H_{c2} can be observed at higher temperatures, but slightly become smeared out. It is interesting to note that well-defined anomalies still exist at 11.1 K well above the superfluid phase determined in Ref. [17]. Above 18 K both anomalies disappear. At 26.5 K the mode c_{11} softens smoothly with field, corresponding to the paramagnetic phase revealed by the magnetization measurements.

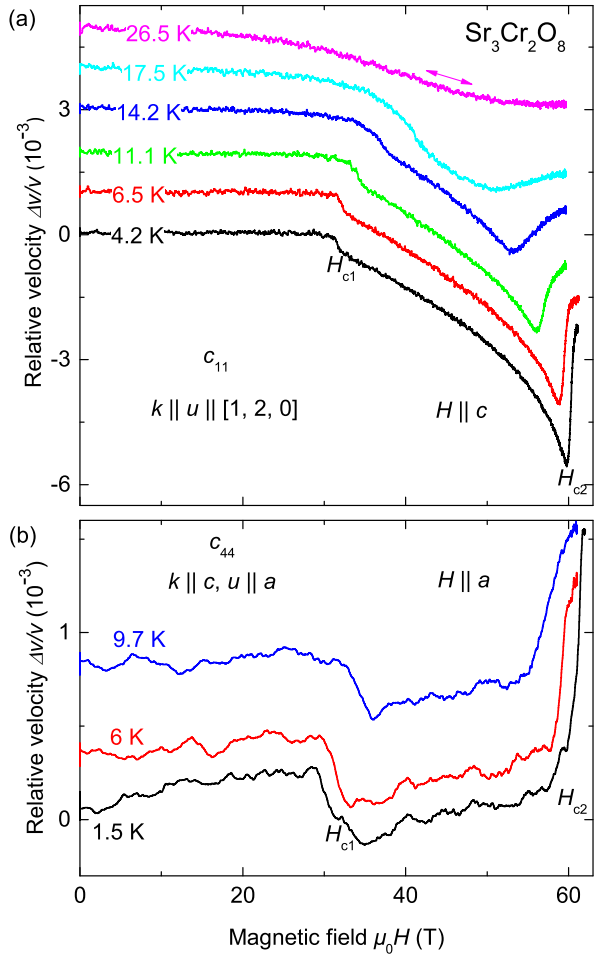

FIG. 3. Sound velocity of (a) the tensile mode c_{11} and (b) the shear mode c_{44} as a function of magnetic field $H\|c$ and $H\|a$ at various temperatures. Results for higher temperatures are shifted by a constant value for clarity.

The shear mode c_{44} exhibits a different field dependence of the relative sound velocity $\Delta v/v$ as shown in Fig. 3(b). At 1.5 K, this mode softens suddenly at the lower critical field H_{c1}. With increasing field, the velocity increases slightly in the 3D XY antiferromagnetic phase till an abrupt hardening appears at H_{c2}. Similar behavior can be also observed at 6 K and at 9.7 K above the superfluid phase. Below 18 K and as a function of temperature, the critical fields are determined by calculating the field derivative of the sound velocity, which are summarized in Fig. 4. Since with increasing temperature the values of H_{c1} and H_{c2} increase and decrease, respectively, an asymmetric domelike phase above the magnonic condensation can be established in the temperature-field representation of Fig. 4.

We argue that the domelike structure with a maximum temperature of $T_{\max} = 18$ K at 47 T is a distinct

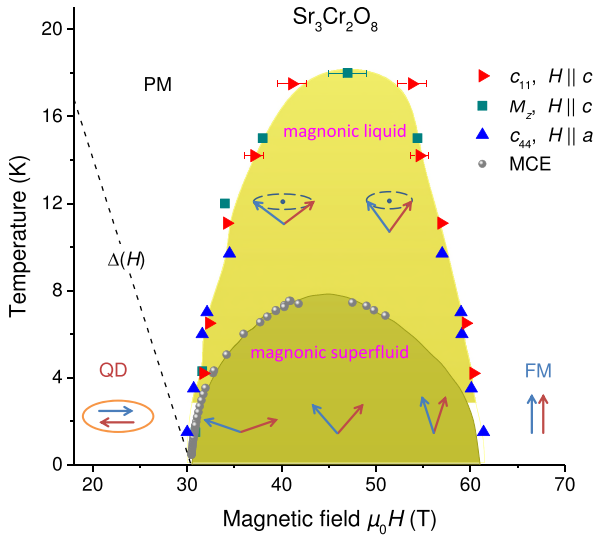

FIG. 4. Temperature versus magnetic field phase diagram of $Sr_3Cr_2O_8$. The magnonic liquid phase is determined by ultrasound and magnetization measurements in this work. The magnonic superfluid is indicated according to the magnetocaloric-effect (MCE) results in Ref. [17]. The pair of arrows stands for the two spins in a dimer. The QD state is represented by a spin-singlet state, the FM state by the parallel alignment of spins. In the magnonic liquid S^z increases with fields and only in the superfluid does the transverse component $S_i^x + iS_i^y$ become coherent.

thermodynamic phase, which can be understood as a magnonic liquid. This liquid establishes an intermediate phase between the magnonic superfluid and the paramagnetic state. At the domelike phase boundary that separates the magnonic liquid from the paramagnetic, the quantum disordered, and the field-induced ferromagnetic phases, we always find the same characteristic anomalies, indicative of thermodynamic phase transitions, probably driven by strong spin-phonon coupling.

Even quantitatively the same value of the sound velocities is reached within the dome below $T_{\max}$, as well as a similar magnetization including its field derivative. While the low-field quantum disorder is manifested by a nonmagnetic spin-singlet state, the high-field ferromagnet is composed of fully polarized spins, the superfluid characterizes coherent XY AFM order, and the magnonic liquid is characterized by a finite magnon density and dominant magnon hopping. The latter requires weaker magnon repulsions compared to their kinetic energies. In this case, a magnonic solid with a commensurate superstructure cannot be stabilized [5]. Experimentally, for magnonic solids fractional-magnetization plateaus are expected, which do not exist in $Sr_3Cr_2O_8$ [Fig. 2(a)].

The similarity of the field-dependent behavior in the sound velocity for temperatures above and below the superfluid phase (Fig. 3) rules out the possibility that the magnetic order that couples to the sound waves can be dominated by the transverse spin component $S^x + iS^y$. Otherwise, distinct anomalies should be observed in the sound velocity when crossing the boundary to the superfluid phase, because the transverse order becomes coherent only within the superfluid dome as revealed by magnetocaloric measurements [17]. This points to the dominant coupling of the longitudinal order S^z to the elastic modes. Hence, it is natural to infer that the magnonic liquid is a phase hosting long-range S^z order, which can be induced by a magnetic field due to frustrated interdimer exchange [31] in the distorted triangular lattice [18,20]. The absence of anomalies at the boundary to the magnonic liquid in the magnetocaloric measurements [17] indicates that the transverse spin degrees of freedom dominate the thermodynamics.

Spin-phonon interactions are usually originating from exchange striction [29,30,32,33]. Via this mechanism the exchange paths are modulated by sound waves, leading to a renormalization of the sound velocity. While the longitudinal waves mainly modify the distance between the magnetic ions, the transverse waves affect the angles spanned by the magnetic and nonmagnetic ions, thus modulating especially indirect exchange. The exchange-striction senario has been elaborated theoretically for longitudinal as well as transverse elastic modes [29,30,32]. In a magnetic field, the sound velocity can be renormalized by the magnetization and/or the magnetic susceptibility, and the renormalization of the sound velocity is proportional to the exchange-striction constants [29,30].

As shown in Figs. 3(a) and 3(b), the tensile c_{11} and shear c_{44} modes are sensitive to the magnetic phase transitions but show different field dependencies in the magnonic-liquid phase. The sound velocity of the c_{11} mode exhibits a field dependence similar to that of the magnetization [Fig. 2(a)], while $\Delta v/v(H)$ for c_{44} resembles that of the magnetic susceptibility [Fig. 2(b)]. The different field dependencies indicate that they are coupled to different orders of magnetization. Phenomenologically, one can infer that the c_{11} and c_{44} modes are coupled to linear and quadratic terms of the magnetization M_z along the field direction, respectively [33,34]. The longitudinal c_{33} mode is also expected to modulate the intradimer exchange but is found to be insensitive to the quantum phase transitions, which documents that the modulation of the exchange integrals by the longitudinal wave along the spin-dimer direction in $Sr_3Cr_2O_8$ is rather weak.

In summary, by studying the temperature and magnetic field dependence of the ultrasound velocity and magnetization, we have provided experimental evidence for the existence of a field-induced magnonic liquid in the 3D spin-dimerized quantum antiferromagnet $Sr_3Cr_2O_8$. Compared to a Tomonaga-Luttinger liquid in the 1D two-leg spin ladder with a strong-rung interaction, the magnonic liquid emerges here not only above the 3D XY antiferromagnetic order but also becomes superfluid in the ordered phase. Similar to the Tomonaga-Luttinger liquid, the characteristic temperature of the magnonic liquid is of the order of the dimer-dimer interactions reflected by the magnon bandwidth. We believe that the field-induced magnonic liquid is a universal quantum spin state in 3D spin-dimerized antiferromagnets.

We would like to thank Adam A. Aczel for providing experimental data and Cristian D. Batista and Tommaso Roscilde for valuable discussions. We acknowledge partial support by the Deutsche Forschungsgemeinschaft via Transregio 80 (Augsburg-Munich-Stuttgart), Project DE 1762/2-1, and also the support of the HLD at HZDR, a member of the European Magnetic Field Laboratory (EMFL).

[1] T. Giamarchi, Int. J. Mod. Phys. B **26**, 1244004 (2012).
[2] B. Thielemann *et al.*, Phys. Rev. B **79**, 020408(R) (2009).
[3] P. Bouillot, C. Kollath, A. M. Läuchli, M. Zvonarev, B. Thielemann, C. Rüegg, E. Orignac, R. Citro, M. Klanjšek, C. Berthier, M. Horvatić, and T. Giamarchi, Phys. Rev. B **83**, 054407 (2011).
[4] V. Zapf, M. Jaime, and C. D. Batista, Rev. Mod. Phys. **86**, 563 (2014).
[5] T. Giamarchi, Ch. Rüegg, and O. Tchernyshyov, Nat. Phys. **4**, 198 (2008).
[6] T. Nikuni, M. Oshikawa, A. Oosawa, and H. Tanaka, Phys. Rev. Lett. **84**, 5868 (2000).

[7] Ch. Rüegg, N. Cavadini, A. Furrer, H.-U. Güdel, K. Krämer, H. Mutka, A. Wildes, K. Habicht, and P. Vorderwisch, Nature (London) **423**, 62 (2003).
[8] E. C. Samulon, Y. Kohama, R. D. McDonald, M. C. Shapiro, K. A. Al-Hassanieh, C. D. Batista, M. Jaime, and I. R. Fisher, Phys. Rev. Lett. **103**, 047202 (2009).
[9] B. Wolf, S. Zherlitsyn, S. Schmidt, B. Lüthi, H. Kageyama, and Y. Ueda, Phys. Rev. Lett. **86**, 4847 (2001).
[10] O. Cépas, K. Kakurai, L. P. Regnault, T. Ziman, J. P. Boucher, N. Aso, M. Nishi, H. Kageyama, and Y. Ueda, Phys. Rev. Lett. **87**, 167205 (2001).
[11] R. M. Eremina, T. P. Gavrilova, A. Günther, Z. Wang, M. Johnsson, H. Berger, H.-A. Krug von Nidda, J. Deisenhofer, and A. Loidl, Eur. Phys. J. B **84**, 391 (2011).
[12] Z. Wang, M. Schmidt, Y. Goncharov, Y. Skourski, J. Wosnitza, H. Berger, H.-A. Krug von Nidda, A. Loidl, and J. Deisenhofer, J. Phys. Soc. Jpn. **80**, 124707 (2011).
[13] A. A. Aczel, Y. Kohama, M. Jaime, K. Ninios, H. B. Chan, L. Balicas, H. A. Dabkowska, and G. M. Luke, Phys. Rev. B **79**, 100409(R) (2009).
[14] M. Kofu, J.-H. Kim, S. Ji, S.-H. Lee, H. Ueda, Y. Qiu, H.-J. Kang, M. A. Green, and Y. Ueda, Phys. Rev. Lett. **102**, 037206 (2009).
[15] M. Kofu, H. Ueda, H. Nojiri, Y. Oshima, T. Zenmoto, K. C. Rule, S. Gerischer, B. Lake, C. D. Batista, Y. Ueda, and S.-H. Lee, Phys. Rev. Lett. **102**, 177204 (2009).
[16] Z. Wang, M. Schmidt, A. Günther, F. Mayr, Y. Wan, S.-H. Lee, H. Ueda, Y. Ueda, A. Loidl, and J. Deisenhofer, Phys. Rev. B **85**, 224304 (2012).
[17] A. A. Aczel, Y. Kohama, C. Marcenat, F. Weickert, M. Jaime, O. E. Ayala-Valenzuela, R. D. McDonald, S. D. Selesnic, H. A. Dabkowska, and G. M. Luke, Phys. Rev. Lett. **103**, 207203 (2009).
[18] D. L. Quintero-Castro, B. Lake, E. M. Wheeler, A. T. M. N. Islam, T. Guidi, K. C. Rule, Z. Izaola, M. Russina, K. Kiefer, and Y. Skourski, Phys. Rev. B **81**, 014415 (2010).
[19] Z. Wang, M. Schmidt, A. Günther, S. Schaile, N. Pascher, F. Mayr, Y. Goncharov, D. L. Quintero-Castro, A. T. M. N. Islam, B. Lake, H.-A. Krug von Nidda, A. Loidl, and J. Deisenhofer, Phys. Rev. B **83**, 201102 (2011); **86**, 039901 (E) (2012).
[20] L. C. Chapon, C. Stock, P. G. Radaelli, and C. Martin, arXiv:0807.0877v2.
[21] D. L. Quintero-Castro, B. Lake, A. T. M. N. Islam, E. M. Wheeler, C. Balz, M. Månsson, K. C. Rule, S. Gvasaliya, and A. Zheludev, Phys. Rev. Lett. **109**, 127206 (2012).
[22] Y. Singh and D. C. Johnston, Phys. Rev. B **76**, 012407 (2007).
[23] A. T. M. N. Islam, D. Quintero-Castro, B. Lake, K. Siemensmeyer, K. Kiefer, Y. Skourski, and T. Herrmannsdorfer, Cryst. Growth Des. **10**, 465 (2010).
[24] Z. Wang, D. Kamenskyi, O. Cépas, M. Schmidt, D. L. Quintero-Castro, A. T. M. N. Islam, B. Lake, A. A. Aczel, H. A. Dabkowska, A. B. Dabkowski, G. M. Luke, Yuan Wan, A. Loidl, M. Ozerov, J. Wosnitza, S. A. Zvyagin, and J. Deisenhofer, Phys. Rev. B **89**, 174406 (2014).
[25] D. Wulferding, P. Lemmens, K.-Y. Choi, V. Gnezdilov, Y. G. Pashkevich, J. Deisenhofer, D. Quintero-Castro, A. T. M. Nazmu Islam, and B. Lake, Phys. Rev. B **84**, 064419 (2011).
[26] R. Truell, C. Elbaum, and B. B. Chick, *Ultrasonic Methods in Solid State Physics*, (Academic Press, New York, 1969).
[27] B. Wolf, B. Lüthi, S. Schmidt, H. Schwenk, M. Sieling, S. Zherlitsyn, and I. Kouroudis, Physica (Amsterdam) **294B**, 612 (2001).
[28] V. Tsurkan, S. Zherlitsyn, S. Yasin, V. Felea, Y. Skourski, J. Deisenhofer, H.-A. Krug von Nidda, J. Wosnitza, and A. Loidl, Phys. Rev. Lett. **110**, 115502 (2013).
[29] O. Chiatti, A. Sytcheva, J. Wosnitza, S. Zherlitsyn, A. A. Zvyagin, V. S. Zapf, M. Jaime, and A. Paduan-Filho, Phys. Rev. B **78**, 094406 (2008).
[30] S. Zherlitsyn, V. Tsurkan, A. A. Zvyagin, S. Yasin, S. Erfanifam, R. Beyer, M. Naumann, E. Green, J. Wosnitza, and A. Loidl, Phys. Rev. B **91**, 060406(R) (2015).
[31] P. Sengupta and C. D. Batista, Phys. Rev. Lett. **98**, 227201 (2007).
[32] M. Tachiki and S. Maekawa, Prog. Theor. Phys. **51**, 1 (1974).
[33] B. Lüthi, *Physical Acoustic in the Solid State*, (Springer-Verlag, Heidelberg, 2005).
[34] H. Schwenk, S. Zherlitsyn, B. Lüthi, E. Morre, and C. Geibel, Phys. Rev. B **60**, 9194 (1999).